Water Practice & Technology

IWA PUBLISHING

Water Practice & Technology Vol 18 No 12, 3109 doi: 10.2166/wpt.2023.205

Process design and optimization of EDTA-biojarosite – a treatment approach in the Box–Behnken framework

Bhaskar S.[a,*], Manoj A.[b], Resmi S. R.[a], Divyashree S.[c] and Sreenivasa M. Y.[c]

[a] Department of Civil Engineering, National Institute of Technology Calicut, Kozhikode, Kerala 673 601, India
[b] Department of Architecture and Planning, National Institute of Technology Calicut, Kozhikode, Kerala 673 601, India
[c] Department of Studies in Microbiology, University of Mysore, Mysuru 570006, Karnataka, India
*Corresponding author. E-mail: baskarmalwanitc@gmail.com

BS, 0000-0002-0203-3629

ABSTRACT

A study was conducted to investigate the performance of biojarosite as a catalyst in Fenton oxidation with and without the presence of the chelating agent ethylene diamine tetra acetic acid (EDTA). The addition of EDTA resulted in increased iron dissolution, confirming the role of EDTA as a chelating agent. The heterogeneous catalytic properties of jarosite were confirmed by the removal efficiencies of 93.5 and 83.4%, with and without EDTA, respectively. The Box–Behnken method was employed as a Design of Experiments tool to identify suitable experimental runs. Both Fenton oxidation and EDTA-based Fenton oxidation were examined separately, with PCP removal being the response variable. In the case of Fenton oxidation, the optimization process resulted in the selection of 0.1–1 g/L of iron catalyst, 100–1,000 mg/L of H_2O_2, and a pH range of 2.5–3.5. On the other hand, for EDTA-based Fenton oxidation, the optimal conditions were determined to be 0.1–1 g/L of iron catalyst, 100–1,000 mg/L of H_2O_2, and a pH range of 6.5–7.5. ANOVA was conducted to analyze the results, and the model fit was examined.

Key words: *Acidithiobacillus ferrooxidans*, EDTA, Fenton oxidation, pentachlorophenol

HIGHLIGHTS

- Application of Box–Behnken design procedure for Fenton's oxidation of pentachlorophenol.
- Use of biojarosite-based catalyst for Fenton's oxidation.
- EDTA-based Fenton's oxidation at near neutral pH.
- Comparison of the efficiency of the process with or without EDTA as a chelating agent.

GRAPHICAL ABSTRACT

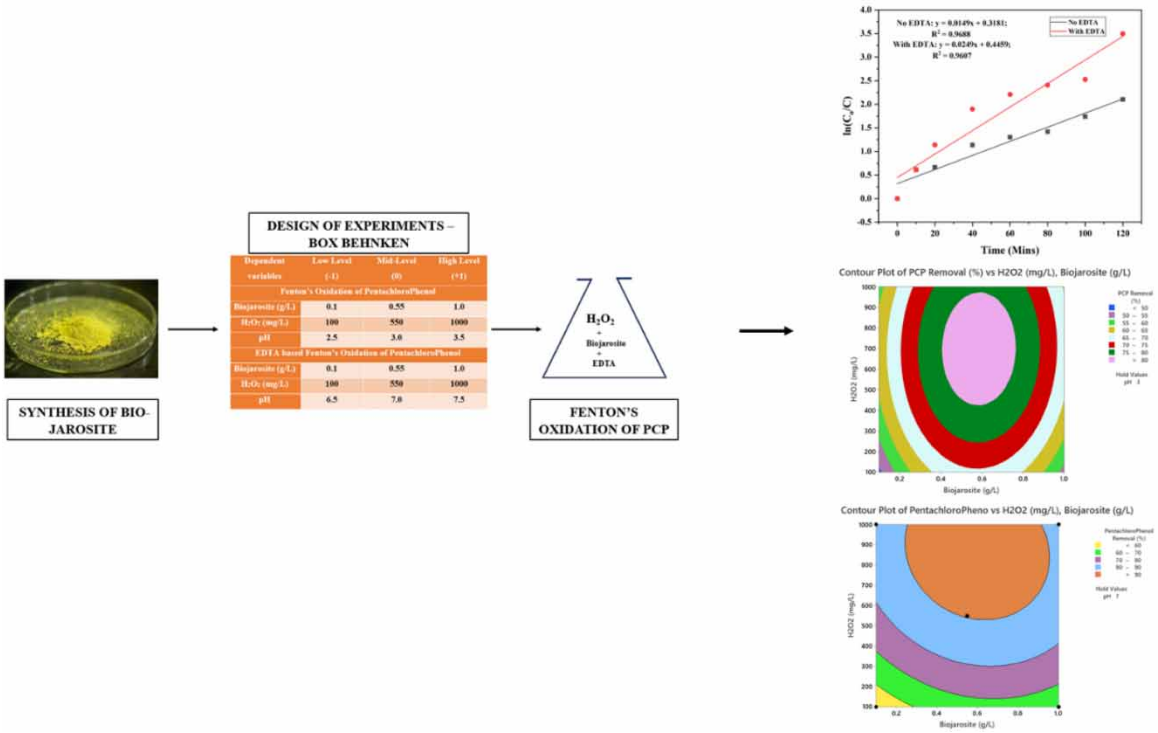

1. INTRODUCTION

The use of pesticides has increased dramatically over the past few decades due to their efficacy in pest control and insect management (Kawahigashi 2009). Pentachlorophenol (PCP), a member of the pentachlorobenzene family of organochlorine pesticides, is composed of an aromatic ring with five chloro groups in place of phenol. As a pesticide and wood preservative, PCP has been widely used in agriculture for many years. However, when PCP leaches out of wood or is carried away by agricultural runoff, it interacts with organic matter in the soil, leading to a decline in fertility (Martınez *et al.* 2000). Depending on the pH-value and presence of solvents, PCP can cause surface and groundwater contamination (Tanjore & Viraraghavan 2016). The inability to trace the non-point sources of pesticide pollution has become a significant environmental concern (Nitschke & Schossler 1998). Due to its toxicity, PCP has been included in the Environmental Protection Agency's list of pollutants (Rodrigues & Kyuma 2013).

Various treatment methods, such as activated carbon adsorption, biological degradation, and advanced oxidation processes, have been extensively explored over the years for the degradation of PCP. Among these techniques, Fenton oxidation has emerged as the most efficient method (Liou *et al.* 2004; Mecozzi *et al.* 2006; Zimbron & Reardon 2009; Rodrigues & Kyuma 2013).

Microporous and mesoporous substances are known for their versatile adsorption. Microporous materials such as zeolites and metal-organic frameworks have pores with sizes on the angstrom order (less than 2 nm). These small pores make them highly selective for the adsorption of molecules of specific size and shape while mesoporous materials with pore sizes between 2 and 50 nm provide a large internal surface area. This large surface area is beneficial for adsorption as it gives the molecules more opportunity to interact with the material (Atiyah *et al.* 2022b, 2022a; Khadim *et al.* 2022).

Fenton oxidation involves the generation of highly reactive hydroxyl radicals, which attack the aliphatic and aromatic components of organic compounds, leading to their decomposition. Numerous researchers have investigated the degradation of PCP using Fenton oxidation (Brown *et al.* 1986; Weavers & Hoffmann 2000; Wolski *et al.* 2006).

In Fenton oxidation, iron, a divalent cation, acts as a catalyst to facilitate the reaction. However, due to cost considerations, alternative catalysts have replaced commercial iron in the treatment process (Bhaskar *et al.*

2019, 2021, 2022b; Bhaskar *et al.* 2020; Rashmishree *et al.* 2022). Mecozzi *et al.* (2006) explored the use of PCP EAF dust as a catalyst for Fenton degradation (Mecozzi *et al.* 2006). In the Fenton oxidation process, Karale *et al.* (2013) introduced an alternative catalyst by substituting chemically leached laterite iron (Karale *et al.* 2013). Similarly, Bhaskar *et al.* (2021) aimed to replace commercial iron with bleached laterite iron in the Fenton oxidation process (Bhaskar *et al.* 2021). Successful attempts have also been made to use biojarosite, an iron hydroxy sulfate, as a catalyst, both in the form of laterite and as a synthesized bioleached laterite nano iron catalyst (Bhaskar *et al.* 2021, 2022a).

The utilization of statistical response surface methodology for process optimization is a recognized approach for developing prediction models. In the context of PCP removal, factorial design has been employed in optimization efforts (Mathialagan & Viraraghavan 2010; Hassen *et al.* 2021). Specifically, A 2^2 factorial design known as Box–Behnken design has been utilized, featuring three interlocking points on the surface sphere surrounding the center, to explore and optimize the impact of key process parameters as independent variables on the response, which serves as the dependent variable (Tripathi *et al.* 2009; Tak *et al.* 2015; Shokri *et al.* 2019). The Box–Behnken design ensures that all design points fall within the selected safe operating zone, providing reliable coefficient estimates close to the center of the design space and eliminating the need for axial points. This design method also enables the identification of significant factors and interactions between variables.

The current study investigates the role of EDTA, acting as a chelating agent, on the dissolution of iron biologically synthesized jarosite in the degradation of pentachloride via Fenton's oxidation process, also evaluating the role of biojarosite as a catalyst in the Fenton's oxidation of PCP at near neutral and acidic pH-value. A comparison is made between this approach and the conventional Fenton oxidation of pentachloride. The regression model is constructed using catalyst loading, H_2O_2 dosage, and pH-value as independent variables, with the removal efficiency of PCP is considered as the response variable.

2. MATERIALS AND METHODS

2.1. Biojarosite catalyzed Fenton oxidation of PCP

The synthesis and characterization of biojarosite were conducted by employing a novel acidophilic strain known as *Acidithiobacillus ferrooxidans* (Accession No. MG271840), following the procedure outlined in a previous study (Bhaskar *et al.* 2019). To investigate the Fenton degradation of PCP catalyzed by biojarosite, two separate experiments were performed with initial target compound concentrations of 10 mg/L, one with the addition of EDTA and the other without EDTA. In each case, biojarosite was gradually added to the Erlenmeyer flask containing the PCP solution, and the pH-value was adjusted to the desired value with 0.5 M H_2SO_4 or 1 M NaOH. The study encompassed a range of experimental conditions, including different dosages of biojarosite (ranging from 0.1 to 1 g/L) and H_2O_2 (ranging from 100 to 1,000 mg/L), separately for the sets with and without EDTA (Bhaskar *et al.* 2022b). Samples were collected at regular intervals for analysis. The concentration of PCP was determined using an HPLC Agilent 1200 system equipped with a C18 reverse phase column (pore size 3.5 μm, 100 × 0.46 cm) and a diode array detector (DAD) (Bhaskar *et al.* 2019). The chemical oxygen demand (COD) was measured using the APHA Method 4500-F: 1992. pH measurements were taken using a digital pH meter (Model – edge, HANNA make). The ferric iron content was determined using the potassium thiocyanate method (Woods & Mellon 1941), while the H_2O_2 concentration was measured using a UV-spectrophotometer (Eisenberg 1943).

2.2. Fenton oxidation of PCP using biojarosite as a catalyst – design of experiment

This study utilized the Box–Behnken design of response surface methodology. The independent variables were chosen at three levels (−1, 0, +1), while the removal of PCP (pentachlorophenol) served as the dependent variable (Table 1). A total of 15 experimental runs were conducted. The variable parameters were optimized within specific ranges: 0.1–1.0 g/L for biojarosite, 100–1,000 mg/L for H_2O_2 dosage, and pH-value ranging from 2.5 to 3.5 without EDTA, and 6.5 to 7.5 with 100 mM EDTA. The focus was on PCP removal, which was considered a countermeasure. Experimental data were used to develop a regression model based on the response, and 3D contour graphs were employed to assess the influential parameters (Bhaskar *et al.* 2022b).

Table 1 | Experimental levels of the variables

Dependent variables	Low level (−1)	Mid-level (0)	High level (+1)
Fenton's oxidation of pentachlorophenol			
Biojarosite (g/L)	0.1	0.55	1.0
H_2O_2 (mg/L)	100	550	1,000
pH	2.5	3.0	3.5
EDTA-based Fenton's oxidation of pentachlorophenol			
Biojarosite (g/L)	0.1	0.55	1.0
H_2O_2 (mg/L)	100	550	1,000
pH	6.5	7.0	7.5

3. RESULTS AND DISCUSSION

3.1. Biojarosite catalyzed Fenton oxidation and EDTA-based Fenton oxidation of PCP

Characterization of biojarosite was discussed in the previous work by Bhaskar and team (2019). The synthesized biojarosite is seen as agglomerated particles resembling rose petals with a smooth interface on scanning electron microscopy and exhibits characteristic peaks on X-ray diffraction (Bhaskar *et al.* 2019). BET surface area observed with biojarosite is 1.62 m^2/g which is consistent (Bhaskar *et al.* 2019; Ali *et al.* 2022a). The removal of PCP was significantly influenced by Fenton oxidation. High removal efficiencies of 93.5 and 83.4% were achieved when using a biojar to H_2O_2 ratio of 1:1 for Fenton oxidation with EDTA and without EDTA, respectively. In the case of Fenton oxidation without EDTA, a degradation rate of about 73.6% was observed within 40 min of treatment. The degradation process continued for 120 min with a rate constant of 0.0142/min, using a catalyst loading of 0.5 g/L. The rate constant exhibited an increase from 0.00594/min to 0.0142/min as the H_2O_2 dosage increased from 100 to 500 mg/L, indicating a higher dissociation of H_2O_2. However, a further increase in H_2O_2 dosage beyond 500 mg/L resulted in a decline in the reaction rate, remaining constant at 0.0050/min, indicating a scavenging effect. When using a catalyst load of 0.1 g/L, a degradation of 62% was observed, while a catalyst load of 0.2 g/L resulted in a degradation of 77.9% within 120 min of treatment. Wang and co-workers (2013) demonstrated that schwertmannite, an iron oxide mineral like jarosite exhibits higher catalytic activity compared to other iron catalysts (Wang *et al.* 2013). Ali and team (2022) conducted the study on the treatment of municipal wastewater using UV-based titanium dioxide catalyst that achieved 95% of turbidity removal (Ali *et al.* 2022b). The highest degradation percentage of 79.5% was achieved with a catalyst load of 1 g/L (Andrades *et al.* 2021) and is illustrated in Figures 1 and 2.

A degradation rate of about 93.5% was achieved for Fenton oxidation with the addition of EDTA, using a catalyst load of 0.5 g/L and an EDTA concentration of 100 mM. The corresponding rate constant was measured at 0.0249/min. It was noted that an increase in degradation occurred with higher H_2O_2 dosages, reaching maximum degradation at an H_2O_2 dosage of 1,000 mg/L, with a rate constant ranging from 0.0126/min to 0.0169/min. EDTA, acting as a chelating agent, possesses carboxylic and amine functional groups that facilitate the complex formation with iron when used in conjunction with an iron catalyst. This interaction aids in the dissociation of iron oxide minerals (Zimbron & Reardon 2009). In the present study, the addition of EDTA accelerated the dissolution of biojarosite, an iron hydroxy sulfate compound. Figure 3 demonstrates that the degradation of PCP increased with the addition of EDTA. Increasing EDTA concentrations from 10, 20, 50, to 100 mM resulted in degradation efficiencies of 66, 78, 80, and 93%, respectively. Previous research also supported the identification of tetrachloro-hydroquinone and dichloromaleic acid as major intermediate compounds in PCP degradation (Zimbron & Reardon 2009). Hu and team (2018) demonstrated that EDTA with iron catalyst helps in the better dissolution of iron thus improving iron reactivity and claimed complete degradation of malachite green dye with EDTA-Iron catalyst (Hu *et al.* 2018).

Figure 4 presents the variation of iron levels during Fenton oxidation. In the investigation without EDTA addition, approximately 189.50 mg/L of iron leached out from biojarosite and participated in the Fenton oxidation process. On the other hand, in the investigation with EDTA addition, a higher amount of total iron, around 257.87 mg/L, leached out and participated in the oxidation.

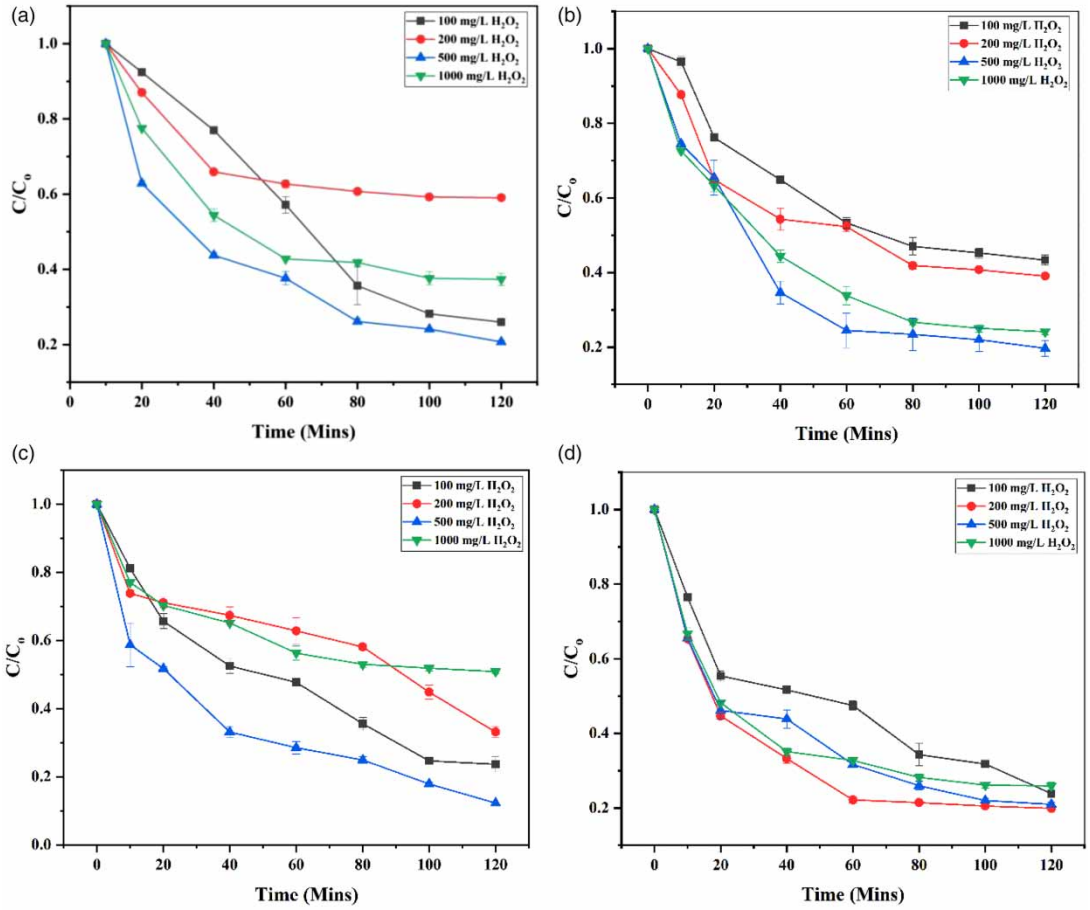

Figure 1 | Degradation of PCP on biojarosite loading without EDTA: (a) 0.1 g/L biojarosite, (b) 0.2 g/L biojarosite, (c) 0.5 g/L biojarosite, and (d) 1.0 g/L biojarosite.

Throughout the study, the pH-value remained slightly acidic, ranging from 3.0 to 4.7, in the absence of EDTA. This acidic pH range favored the oxidation process by promoting the formation of hydroxyl radicals (Kang & Hwang 2000; Burbano *et al.* 2005). The maximum reduction in chemical oxygen demand (COD) observed was 61.23% without EDTA addition and 87.61% with EDTA addition, indicating optimal removal. The adsorption process likely contributed to the removal of organic contaminants, leading to a decrease in COD (Masomboon *et al.* 2009). The leaching of ferrous iron from jarosite directly influenced the oxidation rate. Maximum degradation occurred within the initial 60 min of treatment, after which the process slowed down. The amount of catalyst added also played a role in the heterogeneous Fenton oxidation process, indicating the involvement of adsorption, which contributed to the enhanced removal of target compounds (Boussahel *et al.* 2007; Kang *et al.* 2016; Chen *et al.* 2017). It should be noted that the rate of oxidation in the Fenton process depends on the rate of dissolution of the metallic iron released from the catalyst. The amount of catalyst increases the degradation efficiency due to the adsorption on the surface of the jarosite catalyst particles, making the reaction process heterogeneous (Boussahel *et al.* 2007). Bhaskar *et al.* (2022b) studied the EDTA-based catalytic degradation of dyes using biojarosite, achieving complete dye removal.

According to Fukushima & Tatsumi (2001), tetrachlorocatechol and tetrachloro-hydroquinone were identified as the two major byproducts of Fenton oxidation in the case of PCP. It was observed that at a pH value higher than 5, octachlorodibenzodioxin was formed, while this compound was not detected as an intermediate at pH value 3. The study suggests that the formation of coupling compounds resulting from Fenton oxidation binds with the humic acid used in the experiment, thereby suppressing the formation of octachlorobenzodioxin (Fukushima & Tatsumi 2001).

In another study conducted by Ye and their team (2019), eight intermediates were identified: tetrachlorophenol, trichlorophenol, trichlorohydroquinone, tetrachloro-hydroquinone, hexachlorodibenzobenzofuran, pentachlorodibenzo-*p*-dioxin, hexachlorodibenzo-*p*-dioxin, and octachlorodibenzo-*p*-dioxin. It was proposed that the attack

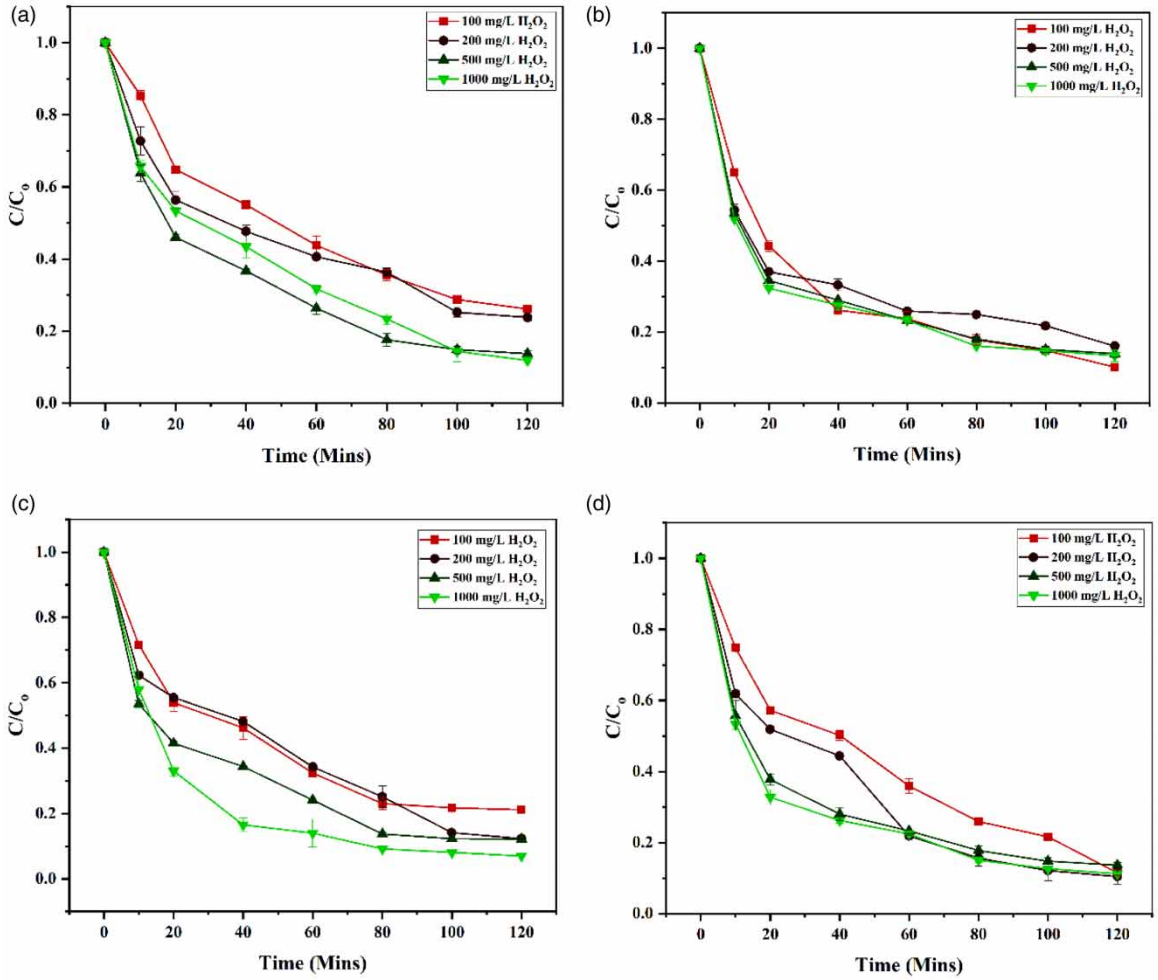

Figure 2 | Degradation of PCP on biojarosite loading with EDTA: (a) 0.1 g/L biojarosite, (b) 0.2 g/L biojarosite, (c) 0.5 g/L biojarosite, and (d) 1.0 g/L biojarosite.

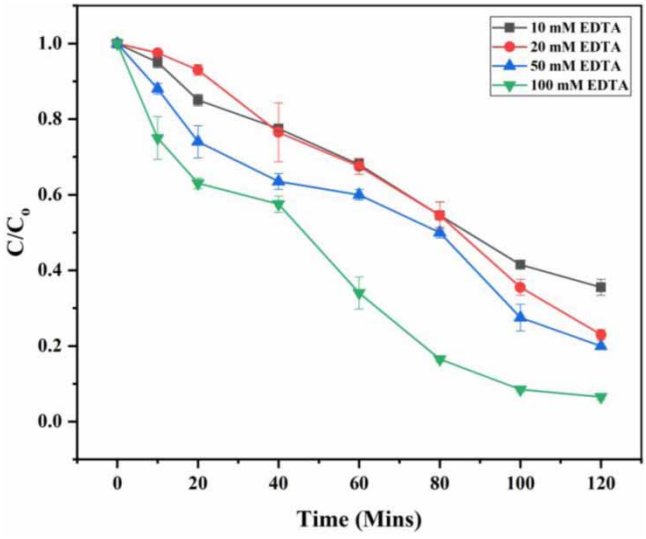

Figure 3 | Effect of EDTA on the Fenton oxidation of PCP with 0.5 g/L of biojarosite loading and 500 mg/L of H_2O_2 dosage.

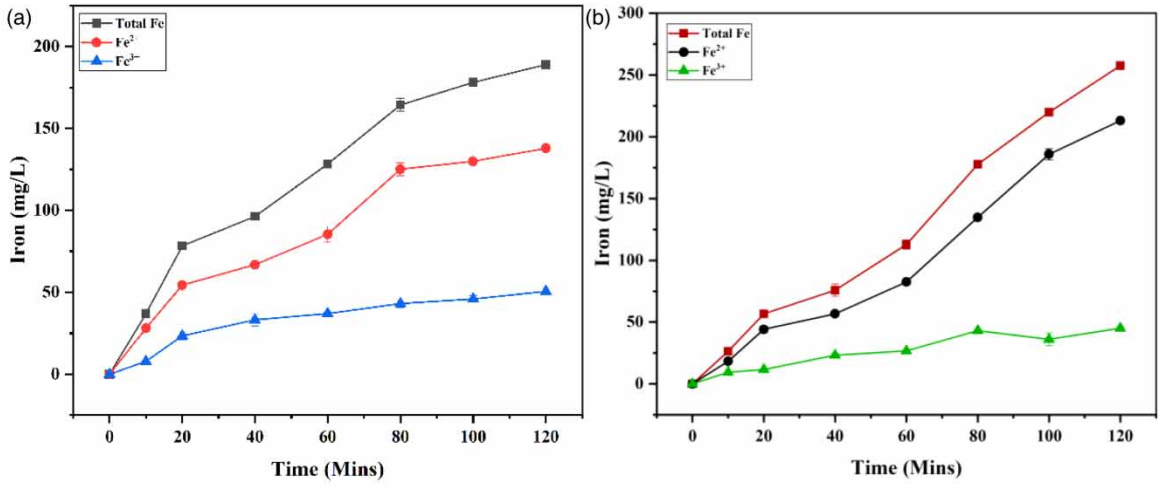

Figure 4 | Variation of iron during the Fenton oxidation of PCP (a) without EDTA and (b) with EDTA.

of hydroxyl radicals (OH•) on aromatic rings led to the formation of hydroxylated products, such as tetrachlorophenol, trichlorophenol, and trichlorohydroquinone. Direct attack of OH• radicals on the Cl–Cl bond resulted in tetrachloroquinone formation. Furthermore, the coupling reaction between PCP radicals formed during Fenton oxidation could lead to the generation of hexachlorodibenzofuran and octachlorodibenzo-*p*-dioxin through further dichlorination processes, resulting in the production of hexachlorodibenzo-*p*-dioxin and pentachlorodibenzo-*p*-dioxin (Ye *et al.* 2019). Thus, mineralization and the formation of dimers from intermediates are significant factors in the degradation of PCP.

Table 2 provides an overview of Fenton degradation, summarizing the key findings. Figure 5 illustrates the linear fit for both Fenton oxidation with and without EDTA. It is observed that both reactions follow pseudo-first-order kinetics. The reuse of catalysts in the degradation of PCP for Fenton oxidation and EDTA-based Fenton oxidation is presented in Table 3.

Table 2 | Overview of Fenton's and EDTA-based Fenton's oxidation of pentachlorophenol optimized

Method	Biojarosite:H_2O_2	pH	PCP removal (%)	COD removal (%)
Fenton's oxidation	1:1	3.0	83.4	61.23
EDTA-based Fenton's oxidation	1:1	7.0	93.5	87.61

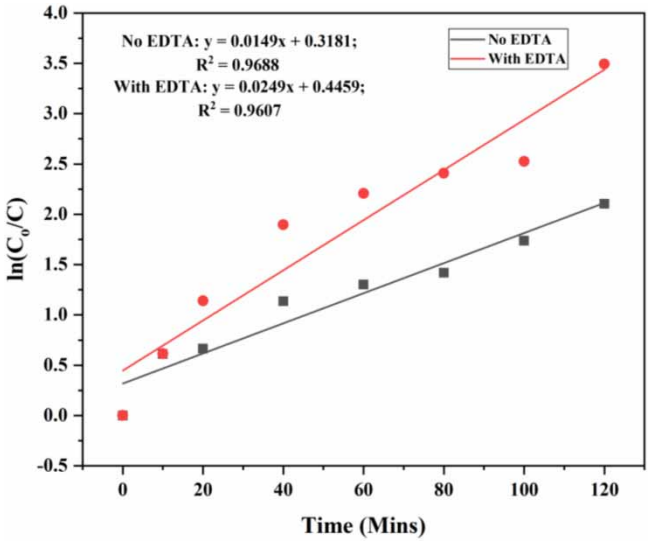

Figure 5 | Linear fit for Fenton oxidation of PCP with and without EDTA.

Table 3 | Reusability of catalyst on Fenton's and EDTA-based Fenton's oxidation of pentachlorophenol

	Fenton's oxidation		EDTA-based Fenton's oxidation	
Cycle	PCP removal (%)	COD removal (%)	PCP removal (%)	COD removal (%)
1	81.5	60.0	89.7	85.5
2	77.0	57.7	79.7	71.2
3	71.5	55.5	72.3	56.5
4	68.6	51.0	69.8	51.7

During the first cycle of reuse, degradation efficiencies of 81.5 and 89.7% were achieved, with corresponding COD removal rates of 60 and 85.5% for Fenton oxidation and EDTA-based Fenton oxidation, respectively. In the second cycle of reuse, the efficiency decreased to 77 and 79.7%, with COD removal rates of 57.7 and 71.2%, respectively. For the third cycle of reuse, degradation efficiencies were measured at 71.5 and 72.3%, with COD removal rates of 55.5 and 56.5%. In the fourth cycle, the degradation efficiencies dropped to 68.6 and 69.8%, with COD removal rates of 51 and 51.7%, respectively. The reuse of the catalyst resulted in a reduction in efficiency by 14.8 and 23.7% for Fenton oxidation and EDTA-based Fenton oxidation of PCP, respectively.

3.2. Fenton oxidation and EDTA-based Fenton oxidation of PCP – design optimization

The significance of PCP removal through Fenton oxidation is indicated by the *F*-value of the model, which is 42.57, with a noise level of 0.03. The model is highly significant, as evidenced by a probability value of <0.0001. The *R*-squared value obtained, 0.9871, indicates a strong correlation between the predicted and observed values, suggesting that 98.71% of the variance can be attributed to the variables, highlighting their high significance in the Fenton oxidation of PCP. The model accounts for 98.71% of the total variance, leaving only 1.29% unexplained. The low probability ($p < 0.0001$) of the *F*-test, along with the ANOVA quadratic regression model, demonstrates that the model is highly significant for the Fenton oxidation of PCP and shows no lack of fit. The lack of fit *F*-value of 11.41 implies that the lack of fit is not significantly related to pure error. There is an 8.16% chance that the lack of fit *F*-value could be attributed to noise. The predicted *R*-squared values of 0.8037 are reasonably close to the adjusted *R*-squared value of 0.9639, with a difference of less than 0.2, indicating good agreement between them (Tables 4 and 5).

Table 4 | ANOVA for the quadratic response surface model fitting for Fenton's oxidation and EDTA-based Fenton's oxidation of pentachlorophenol

	SS	Df	MS	*F*-value	*P*-value	Remarks
Fenton's oxidation of pentachlorophenol						
Residual model	2,008.06	9	223.12	42.57	0.0003	Significant
Lack of fit	24.76	3	8.25	11.41	0.0816	Not Significant
Pure error	1.45	2	0.7233			
Total correlation	2,034.27	14				
$R^2 = 0.9871$ Adjusted $R^2 = 0.9639$ Predicted $R^2 = 0.8034$						
EDTA-based Fenton's oxidation of pentachlorophenol						
Residual model	2,387.40	9	265.27	47.77	<0.0003	Significant
Lack of fit	12.32	3	4.11	0.5316	0.7045	Not Significant
Pure error	15.45	2	7.72			
Total correlation	2145.16	14				
$R^2 = 0.9885$ Adjusted $R^2 = 0.9678$ Predicted $R^2 = 0.9040$						

Table 5 | Coefficient of the model for Fenton's oxidation of pentachlorophenol

Factor	Coefficient estimate	Standard error	*F*-value	*P*-value	Remarks
X	82.57	1.32	42.57	0.0003	Significant
A	2.60	0.8094	10.32	0.0237	Significant
B	5.05	0.8094	38.93	0.0015	Significant
C	−2.35	0.8094	8.43	0.0337	Significant
AB	0.5	1.14	0.1908	0.6805	Not significant
AC	−1.10	1.14	0.1908	0.3804	Not significant
BC	0.15	1.14	0.0172	0.9001	Not significant
A^2	−18.41	1.19	238.72	<0.0001	Significant
B^2	−8.01	1.19	45.18	0.0011	Significant
C^2	−10.66	1.19	80.23	0.0003	Significant

The significance of PCP removal through EDTA-based Fenton oxidation is indicated by the *F*-value of the model, which is 47.77, with a noise level of 0.03 (Table 6). The model is highly significant, as evidenced by a probability value of <0.0001. The *R*-squared value obtained, 0.9885, indicates a high degree of correlation between the predicted and observed values, suggesting that 98.85% of the variance can be attributed to the variables, highlighting their high significance in the EDTA-based Fenton oxidation of PCP. The model accounts for 98.85% of the total variance, leaving only 1.15% unexplained. The ANOVA quadratic regression model demonstrates that the model is highly significant for the EDTA-based Fenton oxidation of PCP, with a low probability ($p <$ 0.0001) for the *F*-test, and it shows no lack of fit. The lack of fit *F*-value of 0.53 implies that the lack of fit is not significantly related to pure error. There is a 70.45% chance that the lack of fit *F*-value could be attributed to noise. The predicted *R*-squared values of 0.9040 show good alignment with the adjusted *R*-squared values of 0.9678, indicating that the difference between them is less than 0.2.

Table 6 | Coefficient of the model for EDTA-based Fenton's oxidation of pentachlorophenol

Factor	Coefficient estimate	Standard error	*F*-value	*P*-value	Remarks
X	90.33	1.36	47.77	0.0003	Significant
A	3.46	0.8331	17.27	0.0089	Significant
B	14.22	0.8331	291.53	<0.0001	Significant
C	1.94	0.8331	4.35	0.0914	Significant
AB	−2.00	1.18	2.88	0.1504	Not significant
AC	−1.38	1.18	1.36	0.2958	Not significant
BC	−0.9	1.18	0.5835	0.4794	Not significant
A^2	−9.10	1.23	55.11	0.0007	Significant
B^2	−9.73	1.23	62.94	0.0005	Significant
C^2	−3.20	1.23	6.83	0.0475	Significant

The coefficient of variance obtained in the Fenton oxidation model is 3.65%, indicating the model's reproducibility. In the case of EDTA-based Fenton oxidation, the coefficient of variance obtained in the model is 3.0%, suggesting possible reproducibility. These low coefficient of variance values demonstrate the high precision and reliability of the experiments conducted in both Fenton oxidation and EDTA-based Fenton oxidation. The *p*-values of the regression coefficients indicate that the linear, quadratic, and interaction effects of the independent variables significantly influence both Fenton oxidation of PCP and EDTA-based Fenton oxidation of PCP. These effects are highly significant, further supporting the robustness of the models.

In the present study, the model terms used for Fenton oxidation of PCP were represented by A, B, C, A^2, B^2, and C^2. The statistical analysis conducted on the experimental data revealed that catalyst loading, H_2O_2 dosage, and pH-value had a significant impact on Fenton oxidation. Specifically, jarosite loading and H_2O_2 dosage exhibited a more linear influence on Fenton oxidation, indicating their contribution to PCP removal. Previous research has also reported a higher positive linear effect of iron dosage compared to H_2O_2 in Fenton oxidation. Moreover, H_2O_2 dosage demonstrated the highest positive linear influence (with a high coefficient) among the variables, surpassing the influences of biojarosite and pH-value. The analysis revealed that the independent variables acted in a quadratic manner, influencing the Fenton oxidation of PCP.

The equation representing the linear regression quadratic model fit is described as follows.

$$Y = 82.57 + 2.60\,A + 5.05\,B - 2.35\,C + 0.5\,AB - 1.10\,AC + 0.15\,BC - 18.41\,A^2 - 8.01\,B^2 - 10.66\,C^2$$

The model terms used for the EDTA-based Fenton oxidation of PCP include A (Biojarosite dosage), B (H_2O_2 dosage), C (pH), A^2, B^2, and C^2. Analysis of the experimental data consistently revealed that both jarosite loading and EDTA addition significantly influenced the UV-Fenton oxidation process. The EDTA-based Fenton oxidation showed a positive correlation with jarosite loading and H_2O_2 dosage, indicating that the removal of PCP was enhanced by increasing jarosite loading and H_2O_2 dosage. Among the variables, H_2O_2 dosage exhibited the highest positive linear influence (coefficient of 14.22), followed by jarosite loading (coefficient of 3.46) and pH-value (coefficient of 1.74). However, the quadratic effect of the independent variables had a negative impact on the oxidation of pentachlorophenol in the EDTA-based Fenton reaction.

The linear regression quadratic equation of the model fit is explained by

$$Y = 90.33 + 3.46\,A + 14.22\,B + 1.74\,C - 2.0\,AB - 1.38\,AC - 0.9\,BC - 9.10\,A^2 - 9.73\,B^2 - 3.20\,C^2$$

In both Fenton oxidation and EDTA-based Fenton oxidation, there is a strong correlation between the actual and predicted responses. The interaction plots for PCP removal by Fenton oxidation and EDTA-based Fenton oxidation are presented in Figures 6 and 7, respectively. It can be observed from Figure 8 that Fenton oxidation

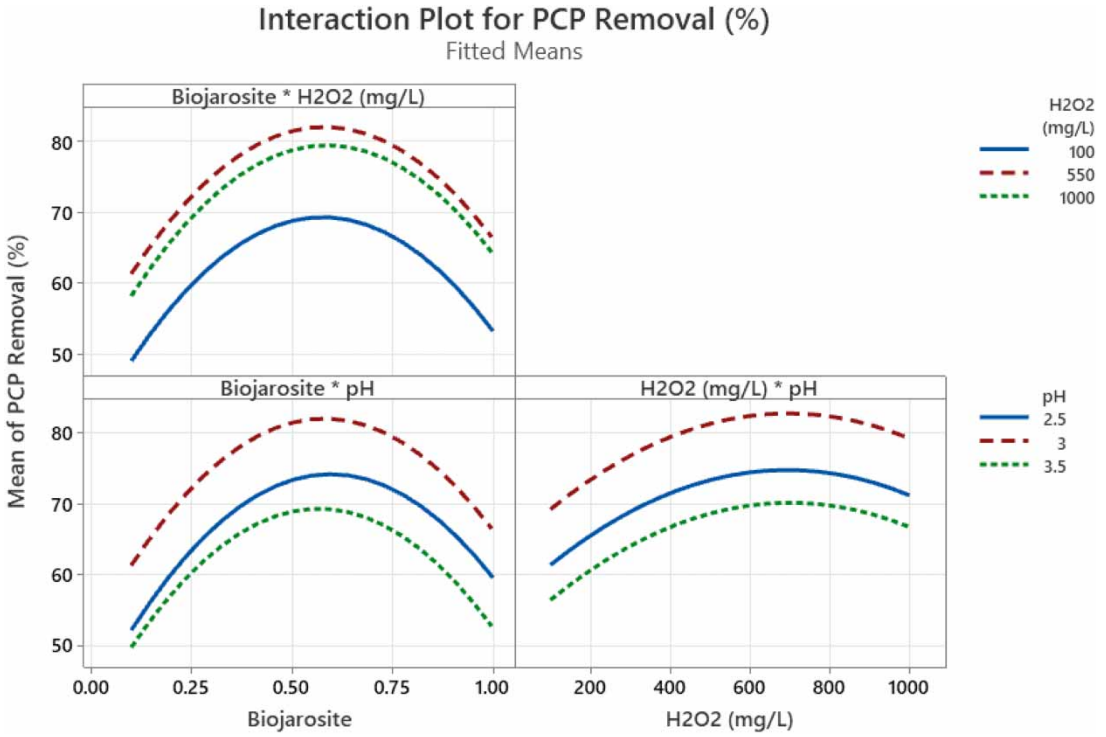

Figure 6 | Interaction plot for PCP removal by Fenton oxidation of PCP.

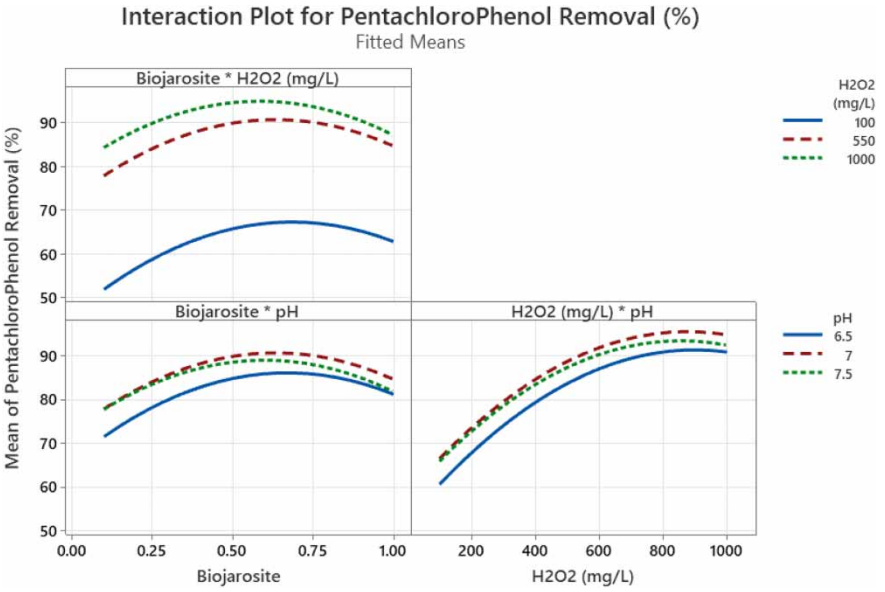

Figure 7 | Interaction plot for PCP removal by EDTA-based Fenton oxidation of PCP.

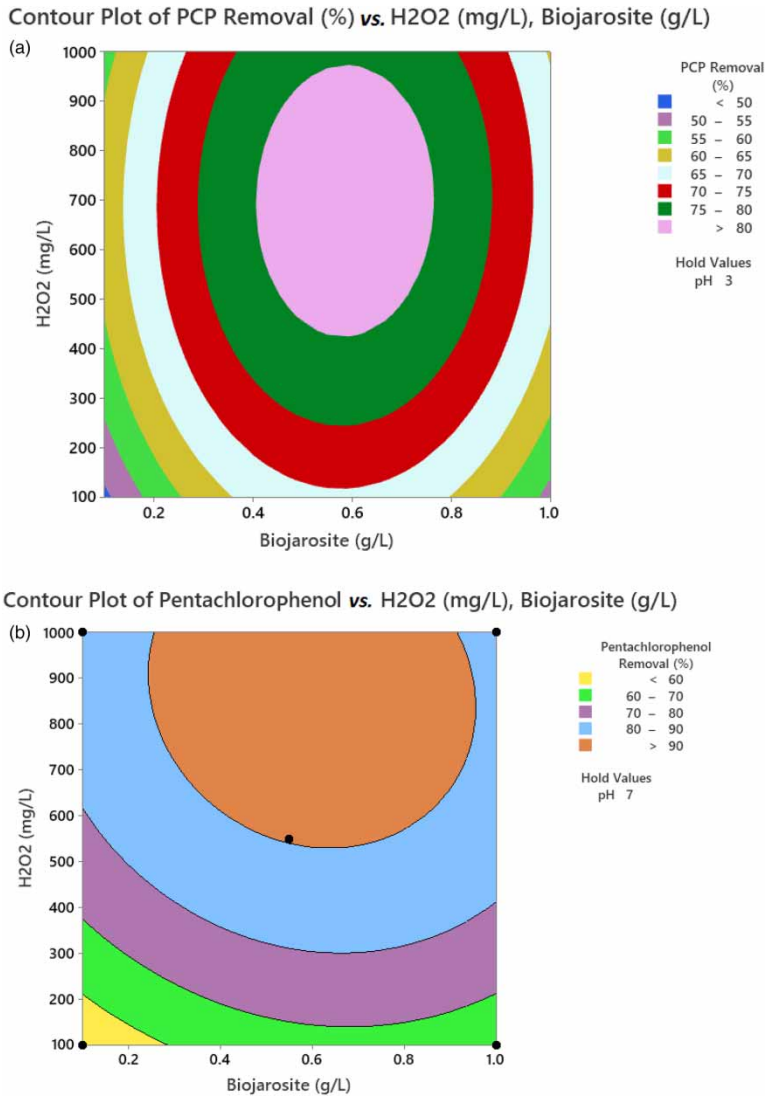

Figure 8 | Contour plot for PCP removal by (a) Fenton oxidation and (b) EDTA-based Fenton oxidation.

for PCP removal operates within a narrow range of biojarosite and H_2O_2 dosages, while EDTA-based Fenton oxidation has a relatively broader range, taking pH-value into consideration. Figure 9 depicts a 3D response surface plot illustrating the Fenton oxidation and EDTA-based Fenton oxidation of PCP.

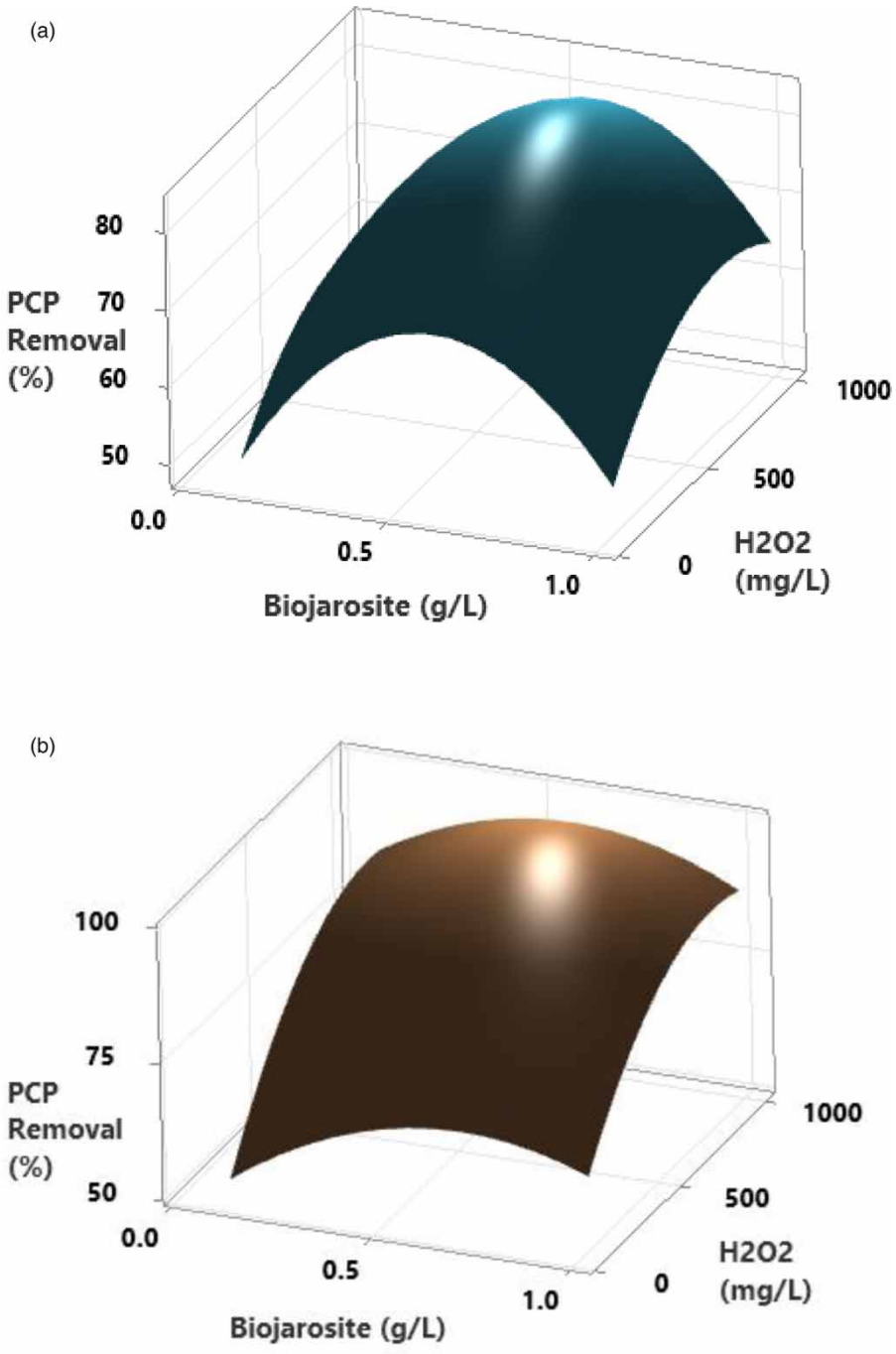

Figure 9 | Response surface 3D plot for PCP removal by (a) Fenton oxidation and (b) EDTA-based Fenton oxidation.

The impact of independent variables on dependent variables was examined through a Pareto chart, as illustrated in Figure 10. For Fenton oxidation, variables B and A exhibited significant effects, while for EDTA-based Fenton oxidation, variables *A*, *B*, and *C* demonstrated significant effects. Specifically, in Fenton oxidation, H_2O_2 dosage was identified as having the greatest influence, whereas in EDTA-based Fenton oxidation, biojarosite loading was found to have the highest effect.

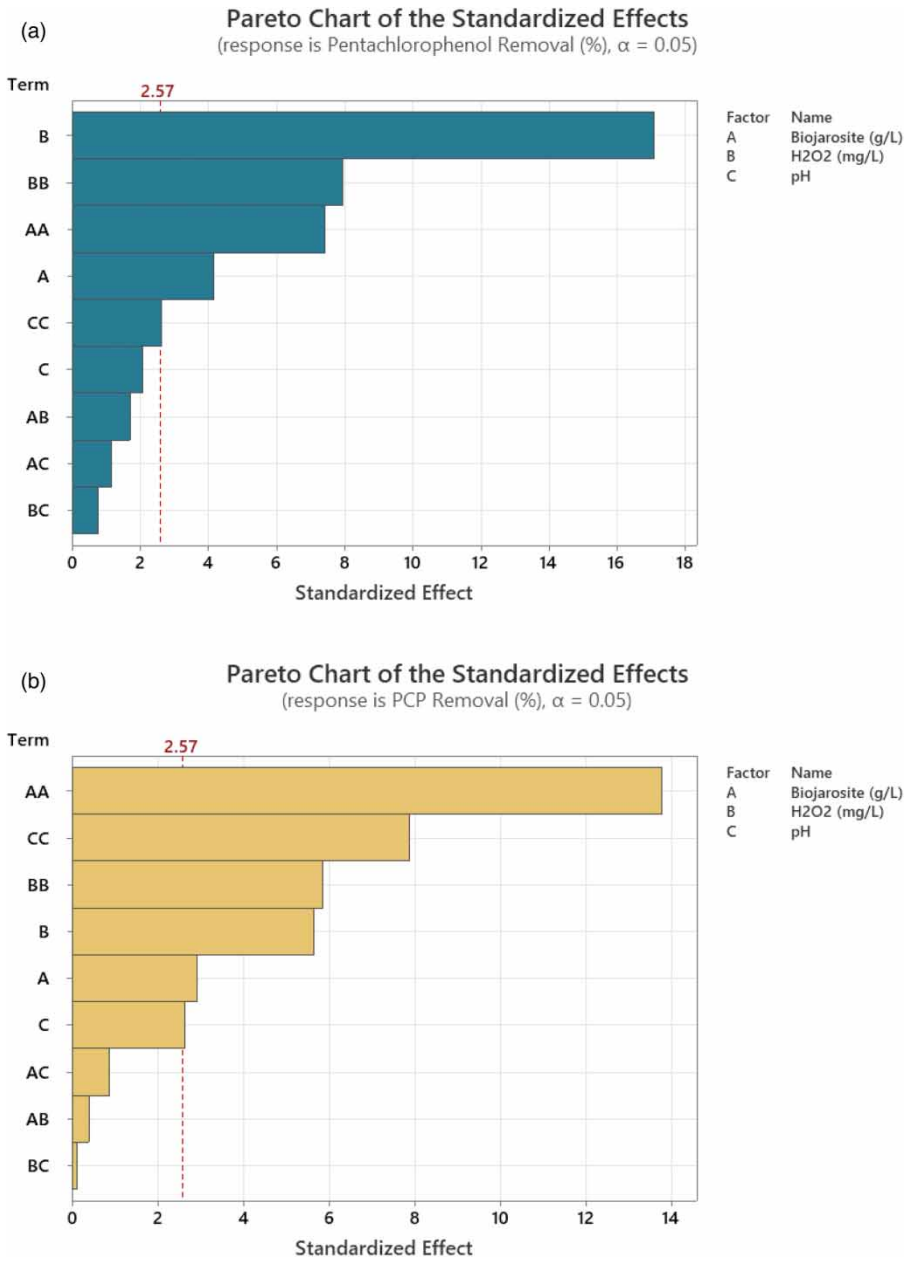

Figure 10 | Pareto chart for PCP removal by (a) Fenton oxidation and (b) EDTA-based Fenton oxidation.

4. CONCLUSIONS

The catalytic efficacy of biojarosite, synthesized from *Acidithiobacillus ferrooxidans*, was assessed in the presence and absence of the chelating agent EDTA, confirming its role. The results indicated that PCP degradation through Fenton oxidation with biojarosite was more pronounced at acidic pH-levels, while at neutral pH-value, the addition of EDTA facilitated the dissolution of iron from biojarosite, enhancing its catalytic activity in PCP degradation. Significant removal efficiencies of 93.5 and 83.4% were observed with and without EDTA, respectively. The degradation of PCP followed a pseudo-first-order reaction with *R*-square values of 0.9607 and 0.9688 for the reactions with and without EDTA, respectively. The efficiency of PCP degradation was further enhanced by increasing the catalyst dosage and H_2O_2 concentration. Both models exhibited excellent fit between the actual and predicted responses, demonstrating the high precision of the Box–Behnken method. The influential parameters were discussed, and quadratic equations were derived for both models. These findings suggest that the utilization of biojarosite as a replacement for commercial iron can enhance the stability of Fenton degradation for organic compounds.

CONSENT TO PUBLISH

All the authors have consented to publish this article

CONSENT TO PARTICIPATE

The authors have consented to participate.

ETHICAL APPROVAL

The authors approve the article for publication.

DATA AVAILABILITY STATEMENT

All relevant data are included in the paper or its Supplementary Information.

CONFLICT OF INTEREST

The authors declare there is no conflict.

REFERENCES

Ali, N. S., Jabbar, N. M., Alardhi, S. M., Majdi, H. S. & Albayati, T. M. 2022a Adsorption of methyl violet dye onto a prepared bio-adsorbent from date seeds: Isotherm, kinetics, and thermodynamic studies. *Heliyon* (8), 10276. https://doi.org/10.1016/j.heliyon.2022.e10276.

Ali, N. S., Kalash, K. R., Ahmed, A. N. & Albayati, T. M. 2022b Performance of a solar photocatalysis reactor as pretreatment for wastewater via UV, UV/TiO_2, and UV/H_2O_2 to control membrane fouling. *Scientific Reports* **0123456789**, 1–10. https://doi.org/10.1038/s41598-022-20984-0.

Andrades, J. A., Coello, M. D., Quiroga, J. M. & Lojo-l, M. 2021 Degradation of simazine by photolysis of hydrogen peroxide Fenton and photo-Fenton under darkness, sunlight and UV light. *Journal of Water Process Engineering* **42**. https://doi.org/10.1016/j.jwpe.2021.102115.

Atiyah, N. A., Albayati, T. M. & Atiya, M. A. 2022a Functionalization of mesoporous MCM-41 for the delivery of curcumin as an anti-inflammatory therapy. *Advanced Powder Technology* **33**(2), 103417. https://doi.org/10.1016/j.apt.2021.103417.

Atiyah, N. A., Albayati, T. M. & Atiya, M. A. 2022b Interaction behavior of curcumin encapsulated onto functionalized SBA-15 as an efficient carrier and release in drug delivery. *Journal of Molecular Structure* **1260**, 132879. https://doi.org/10.1016/j.molstruc.2022.132879.

Bhaskar, S., Manu, B. & Sreenivasa, M. Y. 2019 Bacteriological synthesis of iron hydroxysulfate using an isolated *Acidithiobacillus ferrooxidans* strain and its application in ametryn degradation by Fenton's oxidation process. *Journal of Environmental Management* **232**, 236–242. https://doi.org/10.1016/j.jenvman.2018.11.048.

Bhaskar, S., Basavaraju, Manu & Sreenivasa, M. Y. 2020 Green synthesis of bioleached Flyash iron nanoparticles (GBFFeNP) using *Azadirachta indica* leaves and its application as Fenton's catalyst in the degradation of dicamba. In: Das, B. B., Nanukuttan, S. V., Patnaik, A. K., & Panandikar, N. S. (eds) *Recent Trends in Civil Engineering*, vol. 105, 365–371. Springer, Singapore.

Bhaskar, S., Manu, B. & Sreenivasa, M. Y. 2021 Bioleaching of iron from laterite soil using an isolated *Acidithiobacillus ferrooxidans* strain and application of leached laterite iron as Fenton's catalyst in selective herbicide degradation. *PLoS ONE* **16**. https://doi.org/10.1371/journal.pone.0243444.

Bhaskar, S., Manu, B. & Sreenivasa, M. Y. 2022a Bioleached laterite nano iron catalyst (BLaNFeCs)-based Fenton's degradation of selective dyes in water. *H_2Open Journal* **5**. https://doi.org/10.2166/h2oj.2022.045.

Bhaskar, S., Rashmishree, K. N., Manu, B. & Sreenivasa, M. Y. 2022b Sustainable replacement of EDTA – Biojarosite for commercial iron in the Fenton' s and UV – Fenton' s degradation of Rhowedamine B – a process optimization using Box–Behnken method uncorrected proof. *Water Science and Technology* 1–12. https://doi.org/10.2166/wst.2022.299.

Boussahel, R., Harik, D., Mammar, M. & Lamara-mohamed, S. 2007 Degradation of obsolete DDT by Fenton oxidation with zero-valent iron. *Desalination* **206**(1–3), 369–372. https://doi.org/10.1016/j.desal.2006.04.059.

Brown, E. J., Pignatello, J. J., Martinson, M. M. & Crawford, R. L. 1986 Pentachlorophenol degradation: A pure bacterial culture and an epilithic microbial consortium. *Applied and Environmental Microbiology* **52**(1), 92–97.

Burbano, A. A., Dionysiou, D. D., Suidan, M. T. & Richardson, T. L. 2005 Oxidation kinetics and effect of pH on the degradation of MTBE with Fenton reagent. *Water Research* **39**, 107–118. https://doi.org/10.1016/j.watres.2004.09.008.

Chen, F., Xie, S., Huang, X. & Qiu, X. 2017 Ionothermal synthesis of Fe_3O_4 magnetic nanoparticles as efficient heterogeneous Fenton-like catalysts for degradation of organic pollutants with H_2O_2. *Journal of Hazardous Materials* **322**, 152–162. https://doi.org/10.1016/j.jhazmat.2016.02.073.

Eisenberg, G. M. 1943 Colorimetric determination of hydrogen peroxide. *Industrial and Engineering Chemistry* **15**(5), 327–328. https://doi.org/10.1021/i560117a011.

Fukushima, M. & Tatsumi, K. 2001 Degradation pathways of pentachlorophenol by photo-Fenton systems in the presence of iron (III), humic acid, and hydrogen peroxide. *Environmental Science & Technology* **35**(9), 1771–1778.

Hassen, W., Cherif, H., Werhani, R., Raddadi, N., Neifar, M. & Hassen, A. 2021 Exhaustion of pentachlorophenol in soil microcosms with three *Pseudomonas* species as detoxification agents. *Archives of Microbiology* **203**(7), 4641–4651. https://doi.org/10.1007/s00203-021-02451-y.

Hu, Y., Li, Y., He, J., Kong, L. & Liu, J. 2018 EDTA-Fe (III) Fenton-like oxidation for the degradation of malachite green. *Journal of Environmental Management* **226**, 256–263. https://doi.org/10.1016/j.jenvman.2018.08.029.

Kang, Y. U. N. W. & Hwang, K. 2000 Effects of reaction conditions on the oxidation efficiency in the Fenton process. *Water Research* **34**(10), 2786–2790.

Kang, S., Liu, S., Wang, H. & Cai, W. 2016 Enhanced degradation performances of plate-like micro/nanostructured zero valent iron to DDT. *Journal of Hazardous Materials* **307**, 145–153. https://doi.org/10.1016/j.jhazmat.2015.12.063.

Karale, R., Manu, B. & Shrihari, S. 2013 Catalytic use of laterite iron for degradation of 2-Aminopyridine using advanced oxidation processes. In: *Proceedings of the 'International Conference on Innovations in Civil Engineering ICICE – 2013'*, Kochi, India.

Kawahigashi, H. 2009 Transgenic plants for phytoremediation of herbicides. *Current Opinion in Biotechnology* **20**, 225–230. https://doi.org/10.1016/j.copbio.2009.01.010.

Khadim, A. T., Albayati, T. M. & Saady, N. M. C. 2022 Removal of sulfur compounds from real diesel fuel employing the encapsulated mesoporous material adsorbent Co/MCM-41 in a fixed – bed column. *Microporous and Mesoporous Materials* **341**, 1387–1811.

Liou, R., Chen, S.-H., Hung, M.-Y. & Hsu, C.-S. 2004 Catalytic oxidation of pentachlorophenol in contaminated soil suspensions by Fe^{+3}-resin/H_2O_2. *Chemosphere* **55**(9), 1271–1280. https://doi.org/10.1016/j.chemosphere.2003.12.015.

Martınez, R. C., Fernandez, E. & Sanchez, F. J. 2000 Evaluation of surface- and ground-water pollution due to herbicides in agricultural areas of Zamora and Salamanca (Spain). *Journal of Chromatography A* **869**, 471–480.

Masomboon, N., Ratanatamskul, C. & Lu, M.-C. 2009 Chemical oxidation of 2, 6-dimethylaniline in the Fenton process. *Environmental Science and Technology* **43**(22), 8629–8634.

Mathialagan, T. & Viraraghavan, T. 2010 Biosorption of pentachlorophenol by fungal biomass from aqueous solutions: A factorial design analysis. *Environmental Technology* **2015**, 37–41. https://doi.org/10.1080/09593332608618542

Mecozzi, R., Palma, L. D., Pilone, D. & Cerboni, L. 2006 Use of EAF dust as heterogeneous catalyst in Fenton oxidation of PCP contaminated wastewater. *Journal of Hazardous Materials* **137**, 886–892. https://doi.org/10.1016/j.jhazmat.2006.03.002.

Nitschke, L. & Schossler, W. 1998 Surface water pollution by herbicides from effluents of wastewater treatment plants. *Chemosphere* **36**(l), 35–41.

Rashmishree, K. N., B, S., S, S. & Thalla, A. K. 2022 Extraction of iron from laterite soil and green synthesis of laterite nano iron catalyst (GLaNICs) for its application as Fenton's catalyst in the degradation of triclosan. *Water Science and Technology* **86**(12), 3195–3204. https://doi.org/10.2166/wst.2022.395.

Rodrigues, A. & Kyuma, Y. 2013 Biological Fenton' s oxidation of pentachlorophenol by aquatic plants. *Bulletin of Environmental Contamination and Toxicology* 718–723. https://doi.org/10.1007/s00128-013-1106-4.

Shokri, A., Bayat, A. & Mahanpoor, K. 2019 Employing Fenton-like process for the remediation of petrochemical wastewater through Box–Behnken design method. *Desalination and Water Treatment* **166**, 135–143. https://doi.org/10.5004/dwt.2019.24634.

Tak, B., Tak, B., Kim, Y., Park, Y., Yoon, Y. & Min, G. 2015 Optimization of color and COD removal from livestock wastewater by electrocoagulation process: Application of Box–Behnken design (BBD). *Journal of Industrial and Engineering Chemistry* **28**, 307–315.

Tanjore, S. & Viraraghavan, T. 2016 Pentachlorophenol – water pollution impacts and removal technologies. *International Journal of Environmental Studies* **7233**. https://doi.org/10.1080/00207239408710889.

Tripathi, P., Chandra, V. & Kumar, A. 2009 Optimization of an azo dye batch adsorption parameters using Box-Behnken design. *Desalination* **249**(3), 1273–1279. https://doi.org/10.1016/j.desal.2009.03.010.

Wang, W., Song, J. & Han, X. 2013 Schwertmannite as a new Fenton-like catalyst in the oxidation of phenol by H_2O_2. *Journal of Hazardous Materials* **262**, 412–419. https://doi.org/10.1016/j.jhazmat.2013.08.076.

Weavers, L. K. & Hoffmann, M. R. 2000 Kinetics and mechanism of pentachlorophenol degradation by sonication, ozonation and sonolytic ozonation. *Environmental Science & Technology* **34**(7), 1280–1285.

Wolski, E. A., Murialdo, S. E. & Gonzalez, J. F. 2006 Effect of pH and inoculum size on pentachlorophenol degradation by *Pseudomonas* sp. *Water SA* **32**(1), 93–98.

Woods, J. T. & Mellon, M. G. 1941 Thiocyanate method for iron. *Industrial and Engineering Chemistry Analytical Edition* **13**(8), 551–554.

Ye, Z., Sirés, I., Zhang, H. & Huang, Y. 2019 Mineralization of pentachlorophenol by ferrioxalate-assisted solar photo-Fenton process at mild pH. *Chemosphere* **217**, 475–482. https://doi.org/10.1016/j.chemosphere.2018.10.221.

Zimbron, J. A. & Reardon, K. F. 2009 Fenton's oxidation of pentachlorophenol. *Water Research* **43**(7), 1831–1840. https://doi.org/10.1016/j.watres.2009.01.024.

First received 1 June 2023; accepted in revised form 2 November 2023. Available online 18 November 2023